How to Cite:
Alman, A. A., Soni, V., & Killedar, S. G. (2022). Molecular docking, synthesis and biological evaluation of some Imidazo-thiadiazole based Chalcone derivatives as potent triple mutant T790M/C797S EGFR inhibitors. *International Journal of Health Sciences*, *6*(S2), 14410–14439. https://doi.org/10.53730/ijhs.v6nS2.8781

Molecular docking, synthesis and biological evaluation of some Imidazo-thiadiazole based Chalcone derivatives as potent triple mutant T790M/C797S EGFR inhibitors

Abhinandan A. Alman
Ph.D. Research scholar, B. R. Nahata College of Pharmacy, Department of Pharmacy, Mandsaur University, Mandsaur. Madhya Pradesh, 458001, India
Corresponding author email: nandanvan0088@gmail.com

Vishal Soni
Associate Professor, Faculty of Pharmacy, Mandsaur University, Mandsaur. Madhya Pradesh, 458001, India

Suresh G. Killedar
Professor & Principal, Sant Gajanan Maharaj College of Pharmacy, Mahagaon, Shivaji University, Kolhapur, Maharashtra, 416503, India

***Abstract*---**In present study, we have designed and developed some imidazo-thiadiazole based chalcone derivatives as potential EGFR inhibitors. The designed derivative were screened through molecular docking studies and subjected for synthesis followed by *in vitro* anticancer activity. Most interestingly many molecules had formed one Pi-donor hydrogen bond (Pi-sulfur) or conventional hydrogen bond with Cys797 which is mutated amino acid residue for the second generation EGFR inhibitors. Many molecules had formed Pi-sulfur bond with Met790 which is mutated amino acid residue and developed resistance to the third generation EGFR inhibitors. All the interaction results presented here suggest these molecule has potential to be developed as most potent 4th generation EGFR inhibitors which will might have effectiveness against triple mutant T790M/C797S EGFR. From this investigation, it was decided to synthesize all the designed molecules with their biological evaluation. *In vitro* cytotoxicity of synthesized compounds against MCF-7 (Breast cancer) and A549 (Lung cancer) cells were carried out using MTT assay. All the synthesized compounds induced the cytotoxicity to MCF-7 and A549 and displayed good range of IC_{50} values in between 4 to 59 µm/mL. Against MCF-7, out of all the tested compounds, 10a and 10e exerted good IC_{50} value i.e 4.98 and 9.66 µm/mL, respectively

and compound 10c and 10d shows good IC_{50} value i.e 19.38 and 20.47 µm/mL against A549 respectively. From the present investigation it was observed that synthesized compounds possess enough anticancer potential to treat as novel lead nucleus for the development more potent EGFR inhibitors as fourth generation inhibitors for the treatment of different cancers.

***Keywords*---**EGFR, imidazo-thiadiazole, in vitro anticancer, apoptosis, cell cycle arrest.

Introduction

Although radiotherapy and chemotherapy treat a broad range of tumors indiscriminately, molecular targeting therapies for cancer treatment have the ability to have greater tumor precision. Over the past few decades, significant progress has been made in identifying the complex cellular, biochemical, and genetic pathways that lead to cancer development and progression(Chan et al., 2017). This enhanced mechanistic knowledge of cancer has aided in the design, growth, and clinical testing of more tumor-specific anticancer treatment approaches. Tyrosine kinases are known to play a role in tumor growth and proliferation, and they have become common drug targets. Tyrosine kinase inhibitors (TKIs) prohibit associated kinases from phosphorylating tyrosine residues in their substrates, preventing downstream signaling pathways from being activated(Grünwald & Hidalgo, 2003a). Multiple robust and well-tolerated TKIs targeting single or multiple targets, including EGFR, ALK, ROS1, HER2, NTRK, VEGFR, RET, MET, MEK, FGFR, PDGFR, and KIT, have been developed over the last two decades, contributing to our understanding of precision cancer medicine based on a patient's genetic alteration profile(Song et al., 2016). Some promising cancer treatments have focused on the epidermal growth factor receptor (EGFR) as a molecular target. The EGFR family consists of four transmembrane tyrosine kinases (EGFR1/ErbB1, Her2/ErbB2, Her3/ErbB3, and Her4/ErbB4), as well as thirteen secreted polypeptide ligands(Harari, 2004). EGFRs are overexpressed in multiple solid tumors, including breast, pancreas, head and neck, kidney, vaginal, renal, colon, and non-small-cell lung cancer(Woodburn, 1999). Overexpression of these genes stimulates downstream signaling channels, causing cell proliferation, differentiation, cell cycle progression, angiogenesis, cell motility, and apoptosis inhibition(Chen et al., 2018). If the knowledge of the role of EGFR signaling networks in tumor activity progresses, we would be able to quantify its specific functions more precisely. EGFRs' high expression and/or adaptive activation coincides with the pathogenesis and development of many tumors, making them appealing candidates for both diagnosis and therapy. Several strategies for targeting these receptors and/or the EGFR-mediated effects in cancer cells have been established. EGFRIs are classified into two classes: monoclonal antibodies (mAbs) that specifically target the EGFR extracellular domain, such as cetuximab (Erbitux), and small molecule TKIs that specifically target the EGFR catalytic domain, such as gefitinib (Iressa) and erlotinib (Tarceva)(Ai et al., 2018; Attili et al., 2018; Bryce et al., 2012; Grünwald & Hidalgo, 2003b; Roskoski, 2016).

Chalcones are naturally occurring pharmacologically active compounds which possesses variety of important biological activities. Heterocyclic derivatives of chalcone exhibits anticancer potential against numerous cancer cell lines through different mechanisms. Anticancer chalcone derivatives exhibits and improve the anticancer characteristics by adopting different approaches such as structural and functional manipulation along with substitution of aryl rings(Bhadoriya et al., 2016; Galayev et al., 2015; Gokhale et al., 2017; Lv et al., 2011; Saavedra et al., 2015). Molecular hybridization and replacement in their structure with pharmacological important moieties has been useful for development of novel medicinal agent which shows significant anticancer properties with lesser toxicity. Evolution of new hybrid chalcone analogues occurred through the linkage between efficient chalcone with different adequate and prominent anticancer scaffold like thiadiazole, coumarine, benzothiazole and imidazole which have verified and proved inherent pharmacological role(Akhtar et al., 2017; Ghorab et al., 2015; Gil et al., 2014; Mohana Roopan & Sompalle, 2016). However, chalcones performs a leading appearance in medicinal chemistry but utilization of their pharmacological potential still not enough. ADME features are essential for regulatory approval since they help drug researchers comprehend a medication candidate's safety and effectiveness. A lot of *in silico* models are hence developed for prediction of chemical ADMET properties. However, it is still not easy to evaluate the drug-likeness of compounds in terms of so many ADMET properties(Chaudhari et al., 2020; Khan, Sharuk L; Siddiui, 2020; A. Khan et al., 2022; S. Khan et al., 2021; Sharuk L. Khan et al., 2020, 2021; Shntaif et al., 2021; Siddiqui et al., 2021). In present study, we have designed and developed some imidazo-thiadiazole based chalcone derivatives as potential EGFR inhibitors. The designed derivative were screened through molecular docking studies and subjected for synthesis followed by *in vitro* anticancer activity.

Material and Methods

Parent nucleus and different substitutions

The parent nucleus selected for the development of 3-((2*E*)-3-(2,6-diphenylimidazo[2,1-*b*][1,3,4]thiadiazol-5-yl)acryloyl)-2*H*-chromen-2-one derivatives which was synthesized by three step reaction. The structure of parent nucleus and the different substitutions are tabulated in Table 1 which are already in reference.

Table 1. Parent nucleus and different substitutions of Imidazo-thiadiazole based Chalcone derivatives

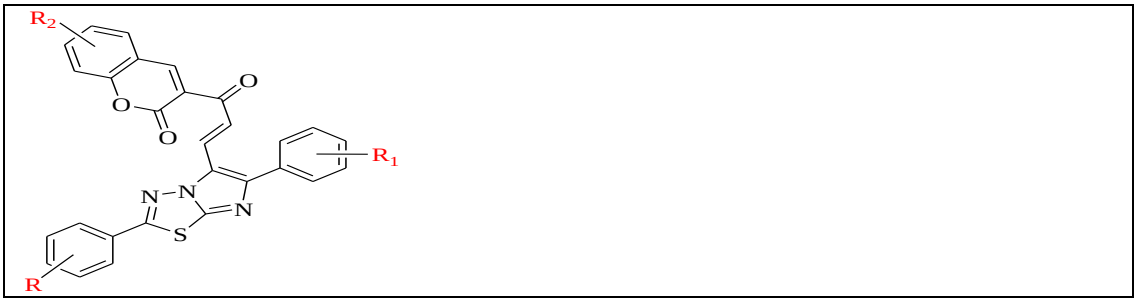

3-((2*E*)-3-(2,6-diphenylimidazo[2,1-*b*][1,3,4]thiadiazol-5-yl)acryloyl)-2*H*-chromen-2-one derivatives			
Code	R	R_1	R_2
10a	H	H	H
10b	H	4-OCH_3	H
10c	H	H	5-Cl
10d	4-Cl	H	H
10e	4-Cl	4-OCH_3	H
10f	4-OCH_3	H	5-Cl
10g	4-OCH_3	H	H
10h	4-NO_2	H	H
10i	4-NH_2	H	H
10j	4-CH_3	H	5-Cl
10k	4-Br	H	H
10l	3-NO_2	H	H
10m	3-NH_2	H	H
10n	2,4-Cl	H	H
10o	3,5-NO_2	H	H
10p	2-I	H	H

Molecular docking

All the selected compounds and the native ligand were docked against the crystal structure of EGFR T790M mutant in complex with naquotinib using Autodock vina 1.1.2 in PyRx 0.8(Dallakyan & Olson, 2015). ChemDraw Ultra 8.0 was used to draw the structures of the compounds and native ligand (mole. File format). All the ligands were subjected for energy minimization by applying Universal Force Field (UFF)(Rappé et al., 1992). The crystal structure of the enzyme with PDB ID 5Y9T was obtained from RCSB Protein Data Bank (PDB) (https://www.rcsb.org/structure/5Y9T). Discovery Studio Visualizer (version-19.1.0.18287) was used to refine the enzyme structure, purify it, and get it ready for docking(San Diego: Accelrys Software Inc., 2012). A three-dimensional grid box (size_x= 55.3036275275Å; size_y= 36.8636912396Å; size_z= 41.8177033184Å) with an exhaustiveness value of 8 was created for molecular docking(Dallakyan & Olson, 2015). BIOVIA Discovery Studio Visualizer was used to locate the protein's active amino acid residues. The approach outlined by Khan et al. was used to perform the entire molecular docking procedure, identify cavity and active amino acid residues(Chaudhari et al., 2020; S. Khan et al., 2021; S.L. Khan et al., 2020; Sharuk L. Khan et al., 2020, 2021; Shntaif et al., 2021; Siddiqui et al., 2021). Fig. 1 shows the revealed cavity of enzyme with the native ligand molecule.

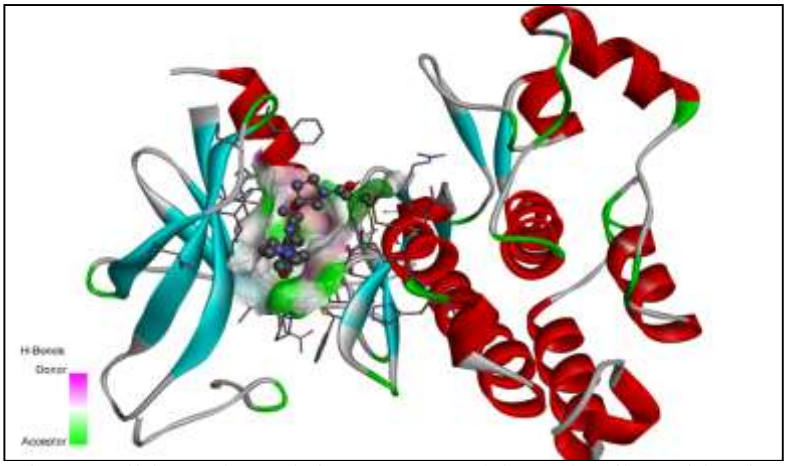

Fig. 1. The 3D ribbon view of the enzyme with native ligand in the cavity

Imidazo-thiadiazole based Chalcone derivatives

All the required chemicals of synthetic grade have been purchased and procured from sigma Aldrich, LOBACHEM and Unique Bilogical and chemicals Kolhapur, Maharashtra, India. The progress of the reaction was confirmed by Thin-layer chromatography [TLC, (Merck precoated silica GF 254)] and compounds were subjected for spectral analysis by ^{1}H, ^{13}C NMR (on a Varian-VXR-300S at 400 MHz NMR spectrometer) and Mass spectroscopy with chloroform (d_6) as the solvent and TMS as the internal standard; chemical shift values were expressed in δ ppm. The melting points were measured using the VEEGO MODEL VMP-D melting point apparatus. The detailed procedure applied for the synthesis of derivatives is illustrated in the section given below.

SCHEME-I

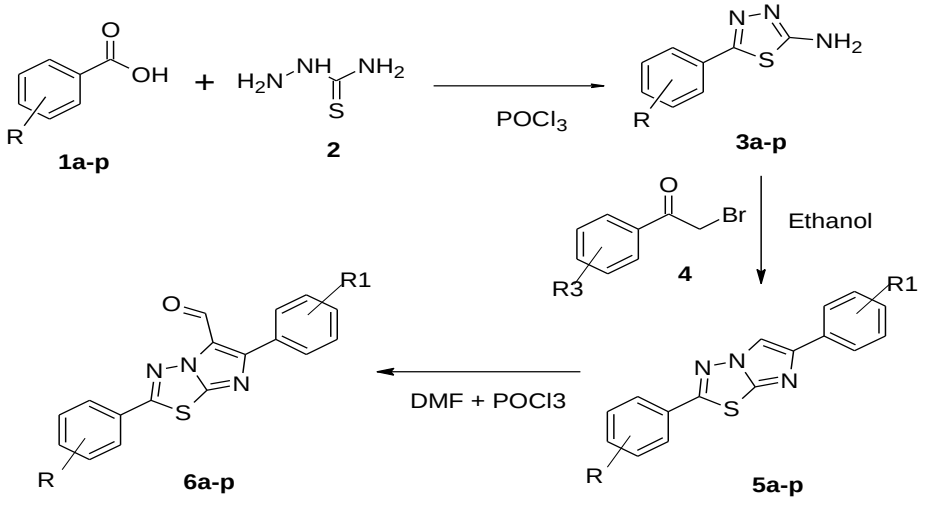

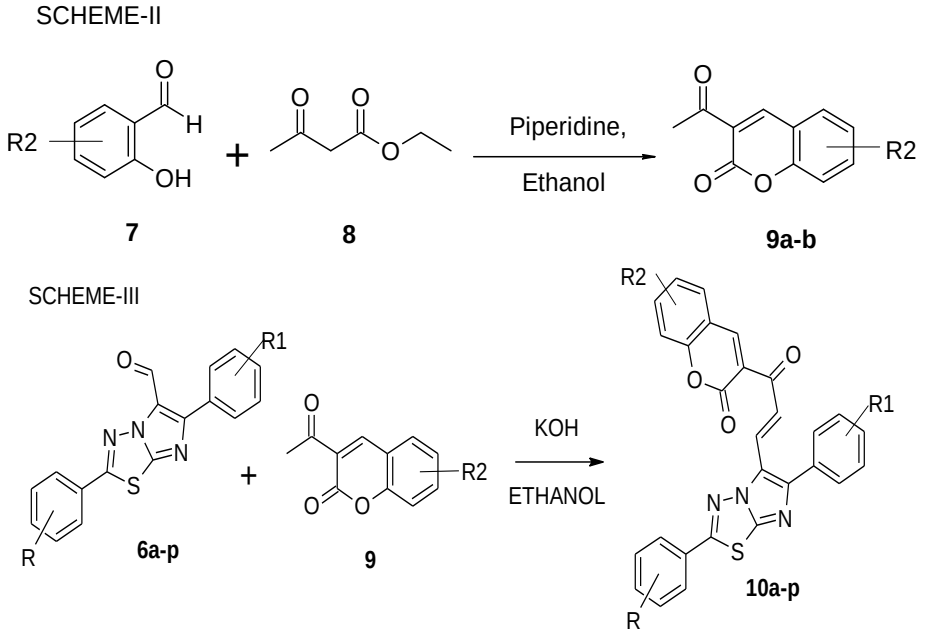

Fig. 2. The reaction scheme for the synthesis of imidazo-thiadiazole based Coumarin derivatives

Experimental

Synthesis of substituted 1,3,4-thiadiazoles(3a-p)

In a mixture of substituted benzoic acid (0.007 mol) and thiosemicarbazide (0.006 mol) add phosphorous oxychloride (0.027 mol) dropwise. The reaction mixture was heat to 85^{0}C for 30 min. cool the mixture, add 7.5ml distilled water and reflux for 4 hours. Resulting mixture was cool at 25-30^{0}C and was basified with 50% NaOH or KOH with drop wise addition under continuous stirring. Separated solid should filter, washed with water and recrystallized with appropriate solvent.

Synthesis of substituted imidazo[2,1-b]-1,3,4-thiadiazoles (5a-p)

A mixture of equimolar quantities of substituted *substituted 1,3,4-thiadiazoles* (0.01 mol) and substituted phenacyl bromides (0.01 mol) was refluxed in dry ethanol for 24 hours. The excess of solvent was distilled off or remove under reduced pressure. The solid hydrobromide salt should collect by filtration, suspend it in water and neutralized by sodium carbonate to get free base. The product was filter, washed with water, dried and recrystallized from suitable solvent

Synthesis of substituted imidazo[2,1-b][1,3,4]-thiadiazole-5-carbaldehydes (6a-p)

Vilsmeier-Haack salt was synthesized by adding phosphorous oxychloride (1.49 ml, 16.06 mmol) drop-wise to a Dimethyl formamide (1.23 ml, 16.06 mmol) maintaining temperature at 0-5^{0}C. Later, a solution of previous step product (2.0

g, 8.032 mmol) in 20 ml of DMF was added to the resulting solution. The reaction mixture was stir at 60^{0}C for about 6 h. The container was cooled and poured into ice cold water with stirring. The solid obtained was filtered, washed with water and then purified by recrystalization using appropriate solvent.

Synthesis of substituted 3-acetyl coumarin (9a-b)

2 ml of piperidine was added to a cold mixture of substituted salicylaldehyde (0.2 mol) and ethylacetoacetate (0.2 mol), with continuous stirring for 20 min. to get yellowish solid. The product was filtered and washed with ethanol and recrystallised from water and ethanol

Synthesis of 7-Substituted-3-{(2E)-3-[2,6-substituted-limidazo[2,1-b][1,3,4]thiadiazol-5-yl]prop-2-enoyl}-2H-chromen-2-one (10a-p)

Equimolar quantities (0.001 mol) of substituted coumarin or simple acetophenones and respective substituted aldehydes (0.001 mol) was mix and dissolved in minimum amount of alcohol. To this, aqueous potassium hydroxide solution (0.003 mol) was add slowly and stir for 2 hrs and was kept for 14-16 hr at room temperature. Resulting reaction mixture was pour into ice water and acidified with dil. HCl. The separated solid was filter and dried and recrystalized from appropriate solvent.

Spectral interpretation of synthesized compounds

Scheme-I product of compound 6a. [2,6-diphenylimidazo[2,1-b][1,3,4]thiadiazole-5-carbaldehyde]

Pale yellow solid, yield: 75%, molecular formula: $C_{17}H_{11}N_3OS$, molecular weight: 305 gm/mol, melting point: 128-131 ^{0}C. Elemental analysis (*cal.*): C, 66.87; H, 3.63; N, 13.76; O, 5.24; S, 10.50. FT-IR (neat, cm^{-1}) ν_{max}: 1251.44 (C-N stretch), 3259.92 (C-H stretch), 1745.60 (C-H bend), 1626.50 (C=O stretch), 1560.52 (C=C stretch), 1376.97 (C-H bend), 617, 681.35, 751.88, 792.68 (aromatic region). MS m/z: 306.23, 307.69 (m+1), 308.87 (m+2), 310.34 (m+3).

Scheme-II - product of compound 9a. [3-acetyl-2H-chromen-2-one]

Off white solid, yield: 89%, molecular formula: $C_{11}H_8O_3$, molecular weight: 188 gm/mol, melting point: 142-144 ^{0}C. Elemental analysis (*cal.*): C, 70.21; H, 4.29; O, 25.51. FT-IR (neat, cm^{-1}) ν_{max}: 3262.19 (C-H stretch), 1740.76 (C-H bend), 1630.65 (C=O stretch), 1568.65 (C=C stretch), 1334.54 (C-H bend), 619, 680.31, 756.89, 798.62 (aromatic region). MS m/z: 189.23, 190.89 (m+1), 192.23 (m+2), 195.87 (m+3).

Scheme-III - 10a. [3-((2E)-3-(2,6-diphenylimidazo[2,1-b][1,3,4]thiadiazol-5-yl)acryloyl)-2H-chromen-2-one]

Yellowish brown solid, yield: 67%, molecular formula: $C_{28}H_{17}N_3O_3S$, molecular weight: 475 gm/mol, melting point: 268-270 ^{0}C. Elemental analysis (*cal.*): C, 70.72; H, 3.60; N, 8.84; O, 10.09; S, 6.74. FT-IR (neat, cm^{-1}) ν_{max}: 1253.32 (C-N

stretch), 3254.49 (C-H stretch), 1750.62 (C-H bend), 1628.85 (C=O stretch), 1568.53 (C=C stretch), 1379.94 (C-H bend), 610, 683.35, 757.38, 782.62 (aromatic region). ^{1}H NMR (300 MHz, CDCl3, chemical shift (ppm)); δ 6-945, 7.112, 7.137, 7.162, 7.185, 7.310, 7.331, 7.404, 7.429, 7.462, 7.524, 7.839, 7.867, 7.894, 8.058, 8.582 (m, Ar-H). ^{13}C NMR (400 MHz, CDCl3, chemical shift (ppm)): δ 122.879, 123.672, 124.209, 125.098, 125.672, 126.029, 126.673, 126.910, 127.172, 128.098, 129.728, 130.452, 131.029, 132.189, 133.712, 134.621, 135.689, 136.019, 143.451, 144.278, 145.902, 150.678, 160.902, 186.902. MS m/z: 476.2, 480.6 (m+2), 482.9 (m+3).

In vitro anticancer activity

The *in vitro* anticancer activity of 16 (10a, 10b, 10c, 10d, 10e, 10f, 10g, 10h, 10i, 10j, 10k, 10l, 10m, 10n, 10o and 10p) compounds were performed on two cancer cell line i.e. MCF-7 (breast cancer) and A549 (lung cancer). Dulbecco`s Modified Eagle Media (DMEM) with low glucose -Cat No-11965-092 (Gibco, invitrogen), Fetal bovine serum (FBS) - Cat No -10270106 (Gibco, invitrogen), antibiotic – antimycotic 100X solution (Thermofisher Scientific)-Cat No-15240062, TACS Annexin V-FITC Apoptosis Detection Kit (R&D Systems) Cat No –4830-01-K, DAPI (D9542), and rhadamine-123 (R8004) were used to perform the anticancer activity.

Cytotoxicity

Cytotoxicity of the compounds were estimated as per the procedure given below:
The cells (MCF-7 and A549) were seeded a 96-well flat-bottom micro plate and maintained at 37°C in 95% humidity and 5% CO_2 for overnight. Different concentration (200, 100, 50, 25, 12.5, 6.25 µl/mL) of synthesized compounds were treated. The cells (MCF-7 and A549) were incubated for another 48 hours. The wells were washed twice with PBS and 20 µL of the MTT staining solution was added to each well and plate was incubated at 37 °C. After 4h, 100 µL of DMSO was added to each well to dissolve the formazan crystals, and absorbance was recorded with a 570 nm using micro plate reader. Using graph Pad Prism Version 5.1, the IC_{50} of compounds were calculated(Kumbar et al., 2021). Surviving cell % was calculated using formula given below:
Surviving cells (%) = Mean OD of test compound /Mean OD of Negative control ×100

Determination of mitochondrial membrane potential

The cells were seeded in a 24-well flat bottom micro plate containing cover slips and maintained at 37 ^{0}C in CO_2 incubator for overnight. Treat 200 µl/mL of respective compounds were treated for 8h.After the treatment, the cells were incubated with Rh-123 dye for 30 min. After the incubation, cells were washed with PBS and fixed with 4% paraformaldehyde for 30 min. Dried cover slips examined under fluorescent microscope(Peram et al., 2019).

DAPI

The cells were seeded in a 24-well flat bottom micro plate containing cover slips and maintained at 37 ^{0}C in CO_2 incubator for overnight. Treat the 200 µl/mL of compounds were treated at 48 hrs. After the incubation, cells were washed with PBS and fixed with 4% paraformaldehyde for 30 min. 20 µL of DAPI was incubated for 5 min at room temperature in the dark, examined under fluorescent microscope. Randomly selecting the fields in the microscope and counted the number of cells undergone apoptosis. Then calculate the percentage of apoptic cells(Bhagwat et al., 2021).

Apoptosis by Flowcytometer

The cells were seeded in a 24-well flat bottom micro plate containing cover slips and maintained at 37 ^{0}C in CO_2 incubator for overnight. The cells 10µg/ml of each sample compound was treated at 48 hrs. After the incubation, cells were washed with PBS and centrifuged for 5 minutes at 500 x g at 4 ^{0}C. Supernatant was discarded, and re-suspended the cell pellets in ice-cold 1X dinding buffer to 1 x 105 per mL. The tubes were kept on ice. Then 1 µL of annexin V-FITC solution and 5 µL PI was added and mixed gently. The tubes were kept on ice and incubated for 15 minutes in the dark. 400 µL of ice-cold 1X binding buffer was added and mixed gently. The cell preparations were analyzed within 30 minutes by flowcytometry(Kumbar et al., 2021; Peram et al., 2019).

Results and Discussion

Molecular docking

The molecular interactions of the compounds with EGFR are tabulated in Table 2. The molecular docking postures of the molecules with receptor are illustrated in Table 3.

Table 2. The binding interactions of the molecules with EGFR

Active amino acid residues	Bond length (kcal/mol)	Bond type	Bond category	Binding energy (kcal/mol)	Docking score
Native ligand					
GLU758	3.88487	Electrostatic	Attractive Charge	568.59	-8.3
GLY857	2.87344	Hydrogen Bond	Conventional Hydrogen Bond		
GLU762	2.10926				
GLU758	3.35859				
GLU758	3.13642		Carbon Hydrogen Bond		
GLU758	3.33922	Electrostatic	Pi-Anion		
GLU762	3.56702				
ALA755	3.69661	Hydrophobic	Alkyl		
PRO877	4.97918				
LEU858	4.28035		Pi-Alkyl		
10a					

ASP855	2.76494	Hydrogen Bond	Conventional Hydrogen Bond	940.63	-9
ARG841	3.03578				
LYS745	2.11014				
ARG841	2.53946				
LYS745	3.29171		Carbon Hydrogen Bond		
ASP837	3.57128	Electrostatic	Pi-Anion		
ASP855	3.97991				
CYS797	4.05727	Hydrogen Bond;Other	Pi-Donor Hydrogen Bond;Pi-Sulfur		
VAL726	3.70616	Hydrophobic	Pi-Sigma		
VAL726	3.95244				
VAL726	3.79866				
MET790	5.50219	Other	Pi-Sulfur		
ARG841	5.29462		Pi-Alkyl		
ARG841	4.98757				
LEU718	5.15859				
ALA743	5.25638				
LEU844	5.24507				
LEU858	5.16532				
10b					
ASP855	2.36689	Hydrogen Bond	Conventional Hydrogen Bond	899.78	9.3
LYS745	2.0832				
CYS797	2.31249				
ARG841	2.73669				
ASP837	3.65116	Electrostatic	Pi-Anion		
CYS797	3.81996	Hydrogen Bond;Other	Pi-Donor Hydrogen Bond;Pi-Sulfur		
VAL726	3.62388	Hydrophobic	Pi-Sigma		
VAL726	3.91721				
VAL726	3.99267				
LEU844	3.85636				
MET790	5.07581	Other	Pi-Sulfur		
MET790	5.86553				
ARG841	5.15646		Pi-Alkyl		
ARG841	4.93797				
LEU718	5.22365				
ALA743	4.69454				
LEU858	5.41268				
10c					
ASP855	2.71433	Hydrogen Bond	Conventional Hydrogen Bond	971.7	9.3
LYS745	2.14858				
ARG841	2.53231				
LYS745	3.54423		Carbon Hydrogen Bond		
ASP837	3.5955	Electrostatic	Pi-Anion		
ASP855	3.99734				
CYS797	4.15361	Hydrogen Bond;Other	Pi-Donor Hydrogen Bond;Pi-Sulfur		
VAL726	3.59106	Hydrophobic	Pi-Sigma		

VAL726	3.92106				
VAL726	3.91931				
LEU844	3.92685				
MET790	5.15794	Other	Pi-Sulfur		
LEU718	3.95312		Alkyl		
ARG841	5.3525				
ARG841	5.02712				
LEU718	5.16318		Pi-Alkyl		
ALA743	4.86709				
LEU858	5.08917				
10d					
ASP855	2.77397				
LYS745	2.23991	Hydrogen Bond	Conventional Hydrogen Bond		
ARG841	2.7089				
LYS745	3.40446		Carbon Hydrogen Bond		
ASP837	3.82716	Electrostatic	Pi-Anion		
ASP855	4.24594				
CYS797	4.06625	Hydrogen Bond;Other	Pi-Donor Hydrogen Bond;Pi-Sulfur		
VAL726	3.56086				
VAL726	3.95332	Hydrophobic	Pi-Sigma	947.43	-9.1
VAL726	3.90509				
LEU844	3.92653				
MET790	5.2089	Other	Pi-Sulfur		
	5.0508				
	4.93885		Pi-Pi Stacked		
LEU858	4.08129		Alkyl		
ARG841	5.20996	Hydrophobic			
ARG841	5.01965		Pi-Alkyl		
LEU718	5.09332				
ALA743	4.90243				
10e					
ASP855	2.61706				
LYS745	1.86743	Hydrogen Bond	Conventional Hydrogen Bond		
LYS745	2.87425		Carbon Hydrogen Bond		
ASP837	3.57385	Electrostatic	Pi-Anion		
ASP855	4.28302				
CYS797	3.89882	Hydrogen Bond;Other	Pi-Donor Hydrogen Bond;Pi-Sulfur		
VAL726	3.72351				
VAL726	3.85289	Hydrophobic	Pi-Sigma	966.02	-9.3
LEU844	3.86621				
MET790	4.92819	Other	Pi-Sulfur		
MET790	5.58787				
	5.42781		Pi-Pi Stacked		
	5.38028	Hydrophobic			
CYS797	4.33355		Alkyl		
LEU858	4.07987				

ARG841	5.20796		Pi-Alkyl		
ARG841	5.07001				
LEU718	5.4291				
ALA743	4.577				
10f					
GLN701	2.28399	Hydrogen Bond	Conventional Hydrogen Bond	1009.92	-8.5
TYR827	2.00834				
ARG831	2.37501				
ILE1018	2.30511				
LEU1017	3.6254		Carbon Hydrogen Bond		
ILE1018	3.59651	Hydrophobic	Pi-Sigma		
	4.08001		Pi-Pi Stacked		
	4.21619				
GLN701, ALA702	4.07726		Amide-Pi Stacked		
LEU778	4.96563		Alkyl		
ILE1018	4.44979				
TYR1016	4.91097		Pi-Alkyl		
10g					
ASP855	2.72463	Hydrogen Bond	Conventional Hydrogen Bond	1013.22	-9.1
LYS745	2.23875				
ARG841	2.68261				
LYS875	3.36824		Carbon Hydrogen Bond		
LYS745	3.37041				
ASP837	3.48628	Electrostatic	Pi-Anion		
ASP855	4.15352				
CYS797	4.15381	Hydrogen Bond;Other	Pi-Donor Hydrogen Bond;Pi-Sulfur		
VAL726	3.53854	Hydrophobic	Pi-Sigma		
VAL726	3.96157				
VAL726	3.94389				
LEU844	3.86542				
MET790	5.09319	Other	Pi-Sulfur		
LEU718	3.94705		Alkyl		
LEU858	4.80849				
PRO877	4.54214				
ARG841	5.24434		Pi-Alkyl		
ARG841	5.09511				
ALA743	5.48132				
LEU718	5.13948				
ALA743	4.80176				
LEU858	5.43799				
10h					
GLN701	2.27345	Hydrogen Bond	Conventional Hydrogen Bond	1023.23	-8.9
TYR1016	2.16693				
TYR827	2.10597				
ARG831	2.34354				
ILE1018	2.31704				

ILE1018	3.68327	Hydrophobic	Pi-Sigma		
GLN701; ALA702	4.12608		Amide-Pi Stacked		
10i					
ASP855	2.77737	Hydrogen Bond	Conventional Hydrogen Bond	945.92	-8.8
LYS745	2.13971				
ARG841	2.556				
LYS745	3.41615		Carbon Hydrogen Bond		
ASP837	3.78594	Electrostatic	Pi-Anion		
ASP855	4.04354				
CYS797	4.06243	Hydrogen Bond;Other	Pi-Donor Hydrogen Bond;Pi-Sulfur		
VAL726	3.69966	Hydrophobic	Pi-Sigma		
VAL726	3.97919				
VAL726	3.76014				
MET790	5.57862	Other	Pi-Sulfur		
ARG841	5.29442		Pi-Alkyl		
ARG841	4.98724				
LEU718	5.13924				
ALA743	5.32892				
LEU844	5.26501				
LEU858	5.33136				
10j					
ASP855	2.77453	Hydrogen Bond	Conventional Hydrogen Bond	978.15	-9.2
LYS745	2.2193				
ARG841	2.70538				
LYS745	3.38755		Carbon Hydrogen Bond		
ASP837	3.63326	Electrostatic	Pi-Anion		
ASP855	4.23613				
CYS797	4.0991	Hydrogen Bond;Other	Pi-Donor Hydrogen Bond;Pi-Sulfur		
VAL726	3.55486	Hydrophobic	Pi-Sigma		
VAL726	3.94759				
VAL726	3.93343				
LEU844	3.8922				
MET790	5.1301	Other	Pi-Sulfur		
LEU858	4.10158		Alkyl		
ARG841	5.25469		Pi-Alkyl		
ARG841	5.05965				
LEU718	5.12986				
ALA743	4.82857				
LEU844	5.48823				
LEU858	5.49643				
10k					
ASP855	2.82367	Hydrogen Bond	Conventional Hydrogen Bond	949.86	-8.9
LYS745	2.14388				
ARG841	2.72206				
LYS745	3.38435		Carbon Hydrogen Bond		

ARG841	4.75617	Electrostatic	Pi-Cation		
ASP837	3.8975		Pi-Anion		
ASP855	4.27778				
CYS797	4.11228	Hydrogen Bond;Other	Pi-Donor Hydrogen Bond;Pi-Sulfur		
VAL726	3.59568	Hydrophobic	Pi-Sigma		
VAL726	3.92647				
VAL726	3.92542				
LEU844	3.91658				
MET790	5.16419	Other	Pi-Sulfur		
ARG841	5.24747		Pi-Alkyl		
ARG841	5.04515				
LEU718	5.16248				
ALA743	4.85551				
10l					
ASP855	2.80587	Hydrogen Bond	Conventional Hydrogen Bond	1052.09	-9
LYS745	2.24061				
ARG841	2.57007				
ARG841	2.33804				
LYS745	3.56218		Carbon Hydrogen Bond		
ASP837	3.60196	Electrostatic	Pi-Anion		
ASP855	4.09575				
CYS797	4.14934	Hydrogen Bond;Other	Pi-Donor Hydrogen Bond;Pi-Sulfur		
VAL726	3.54335	Hydrophobic	Pi-Sigma		
VAL726	3.95912				
VAL726	3.84698				
LEU844	3.9528				
MET790	5.26938	Other	Pi-Sulfur		
ARG841	5.31308		Pi-Alkyl		
ARG841	5.06644				
LEU718	5.09483				
ALA743	4.9733				
LEU858	5.27636				
10m					
ASP855	2.81966	Hydrogen Bond	Conventional Hydrogen Bond	984.37	-8.9
LYS745	2.203				
ARG841	2.55706				
LYS745	3.44883		Carbon Hydrogen Bond		
ASP837	3.54102	Electrostatic	Pi-Anion		
ASP855	4.03159				
CYS797	4.14947	Hydrogen Bond;Other	Pi-Donor Hydrogen Bond;Pi-Sulfur		
VAL726	3.59662	Hydrophobic	Pi-Sigma		
VAL726	3.95295				
VAL726	3.8336				
MET790	5.33886	Other	Pi-Sulfur		
ARG841	5.35737		Pi-Alkyl		

ARG841	5.0719				
LEU718	5.10369				
ALA743	5.08656				
LEU844	5.187				
LEU858	5.12378				
10n					
GLN701	2.34124	Hydrogen Bond	Conventional Hydrogen Bond	975.23	-8.8
TYR827	1.93948				
ARG831	2.47422				
ARG776	4.95974	Electrostatic	Pi-Cation		
ILE1018	3.73622	Hydrophobic	Pi-Sigma		
GLN701;ALA702	4.0548		Amide-Pi Stacked		
LEU778	5.43747		Alkyl		
ILE1018	4.34858				
TYR1016	5.0948		Pi-Alkyl		
10o					
TYR1016	3.36681	Hydrogen Bond	Conventional Hydrogen Bond	1071.31	-9.1
TYR1016	2.9096				
ASN700	2.57431				
ARG705	2.971				
TYR827	1.86204				
ARG831	2.7943				
ILE1018	2.06524				
ILE1018	3.70349	Hydrophobic	Pi-Sigma		
10p					
ASP855	2.95438	Hydrogen Bond	Conventional Hydrogen Bond	997.68	-9
LYS745	2.23356				
ARG841	2.73259				
LYS745	3.44984		Carbon Hydrogen Bond		
ASP855	4.22882	Electrostatic	Pi-Anion		
CYS797	4.08341	Hydrogen Bond;Other	Pi-Donor Hydrogen Bond;Pi-Sulfur		
VAL726	3.55791	Hydrophobic	Pi-Sigma		
VAL726	3.97251				
VAL726	3.94296				
LEU844	3.86789				
MET790	5.12867	Other	Pi-Sulfur		
PHE723	5.74164		Pi-Pi T-shaped		
ARG841	5.38967		Pi-Alkyl		
ARG841	5.08964				
LEU718	5.13956				
ALA743	4.83843				
LEU844	5.48785				
PHE723	5.49543				

Table 3. The 2D-and 3D molecular docking postures of the molecules with EGFR

3D docking pose	2D docking pose
Native ligand	
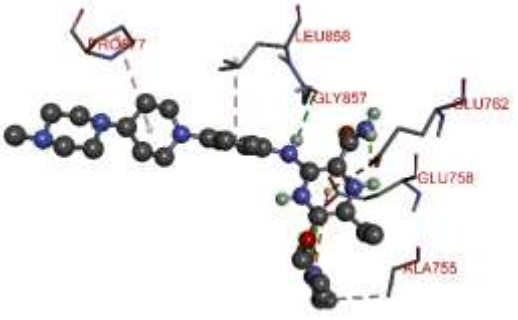	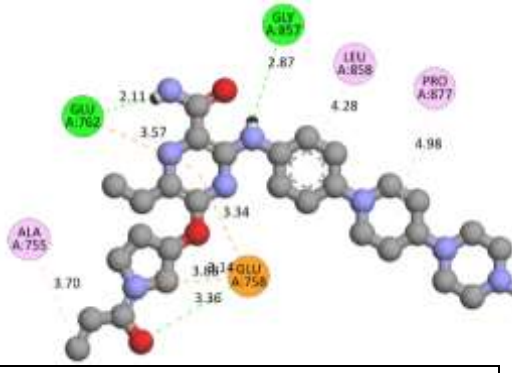
10a	
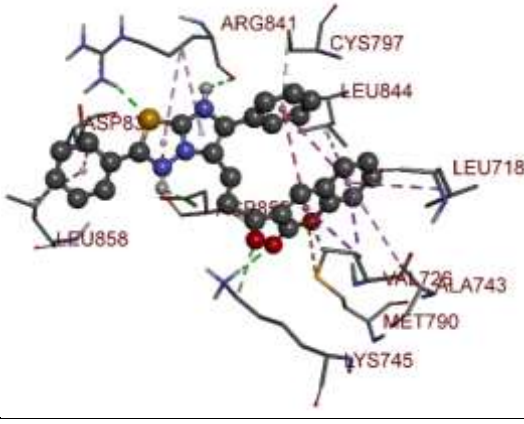	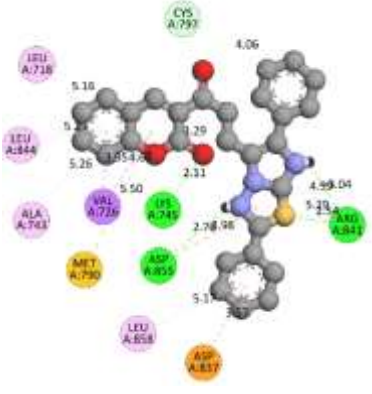
10b	
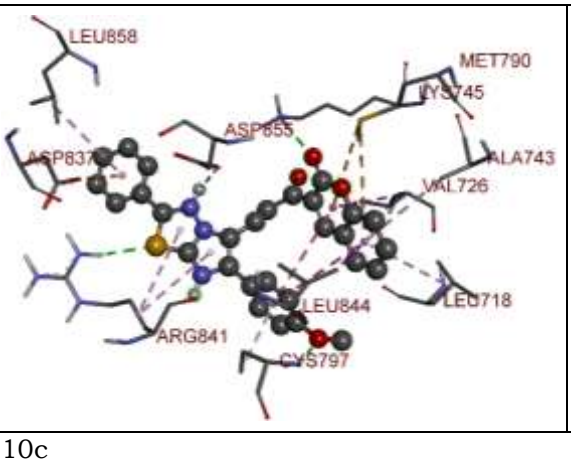	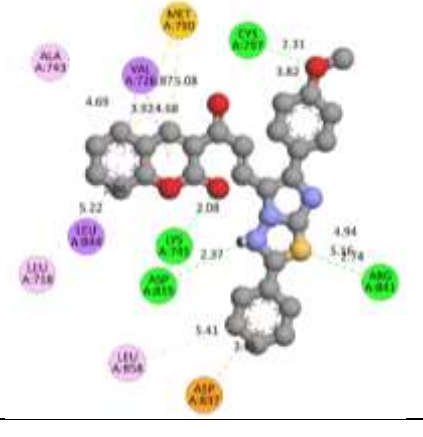
10c	

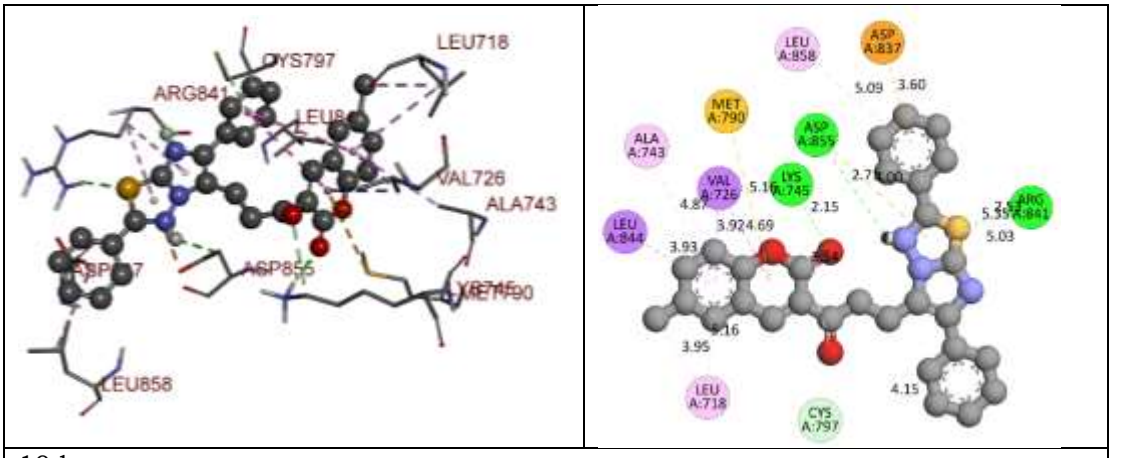
CYS797
LEU718
ARG841
VAL726
ALA743
ASP855
LEU858
LEU
A:858
ASP
A:837
MET
A:790
ASP
A:855
ALA
A:743
VAL
A:726
LYS
A:745
LEU
A:844
ARG
A:841
LEU
A:718
CYS
A:797

10d

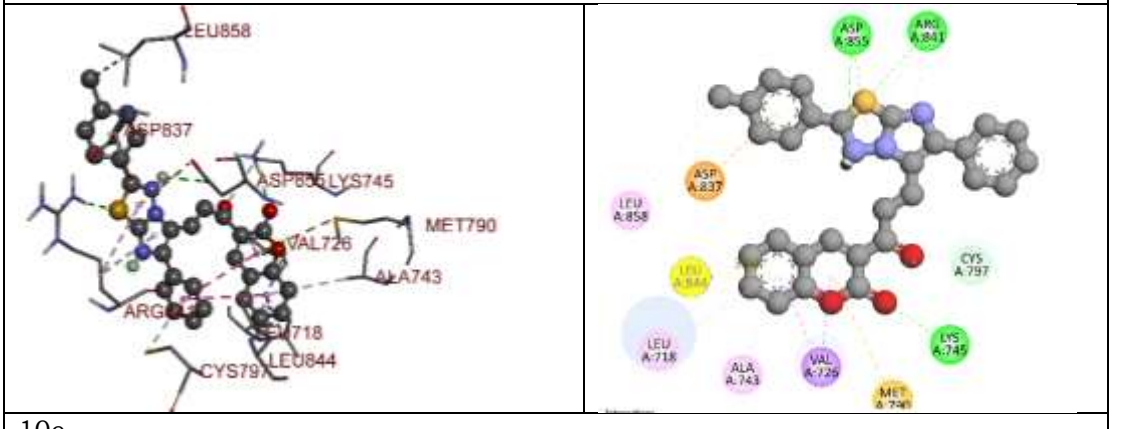
LEU858
ASP837
LYS745
MET790
VAL726
ALA743
LEU718
LEU844
ASP
A:855
ARG
A:841
ASP
A:837
LEU
A:858
CYS
A:797
LEU
A:718
VAL
A:726
ALA
A:743
LYS
A:745

10e

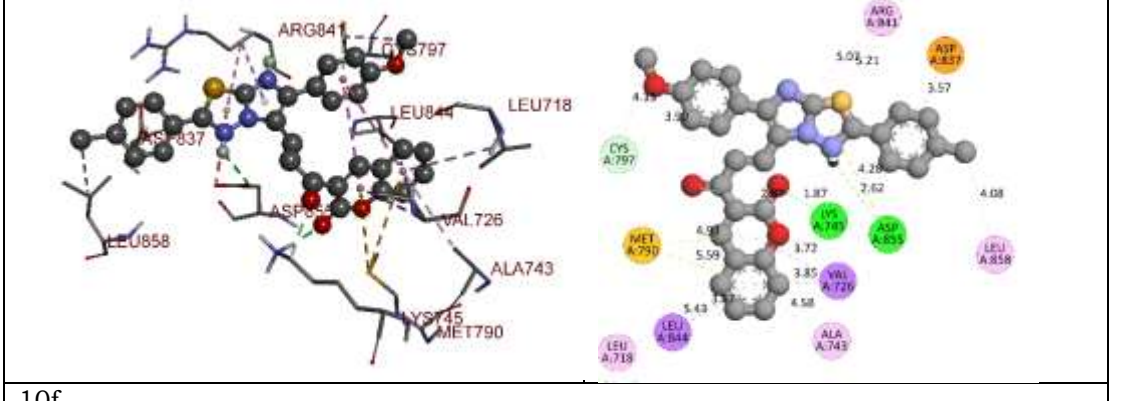
ARG841
LEU844
LEU718
VAL726
LEU858
ALA743
LYS745
MET790
ARG
A:841
ASP
A:837
CYS
A:797
MET
A:790
LYS
A:745
ASP
A:855
LEU
A:858
VAL
A:726
LEU
A:844
ALA
A:743
LEU
A:718

10f

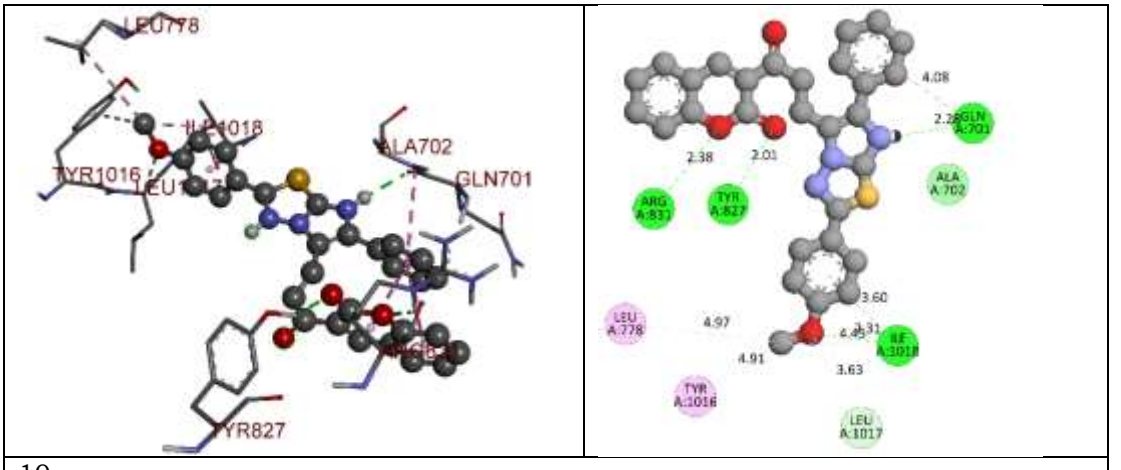
LEU778
ILE1018
TYR1016
LEU
ALA702
GLN701
TYR827
4.08
2.28
GLN A:701
2.38
2.01
ALA A:702
ARG A:831
TYR A:827
3.60
LEU A:778
4.97
4.91
3.63
ILE A:1018
TYR A:1016
LEU A:1017

10g

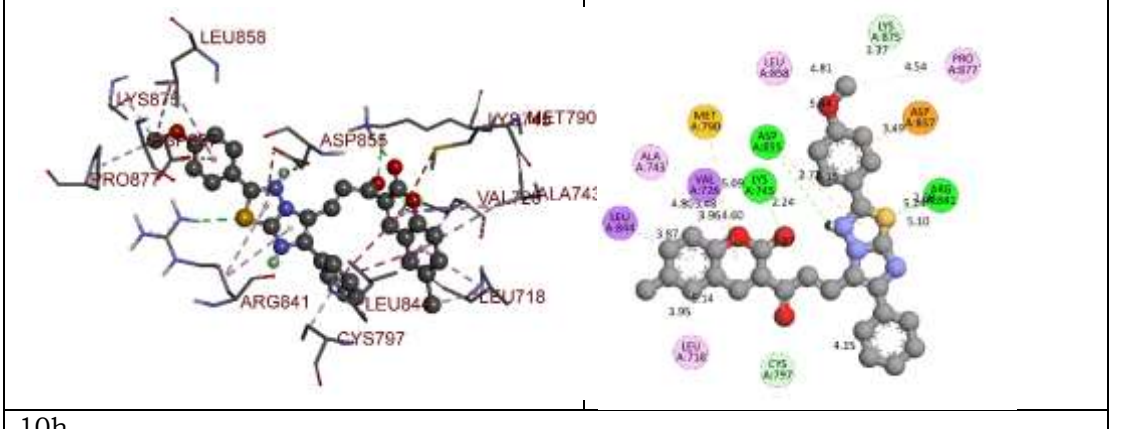
LEU858
LYS875
ASP855
MET790
PRO877
ALA743
ARG841
LEU718
CYS797
LYS A:875
LEU A:858
PRO A:877
MET A:790
ASP A:855
ASP A:837
ALA A:743
LEU A:841
ARG A:842
LEU A:718
CYS A:797

10h

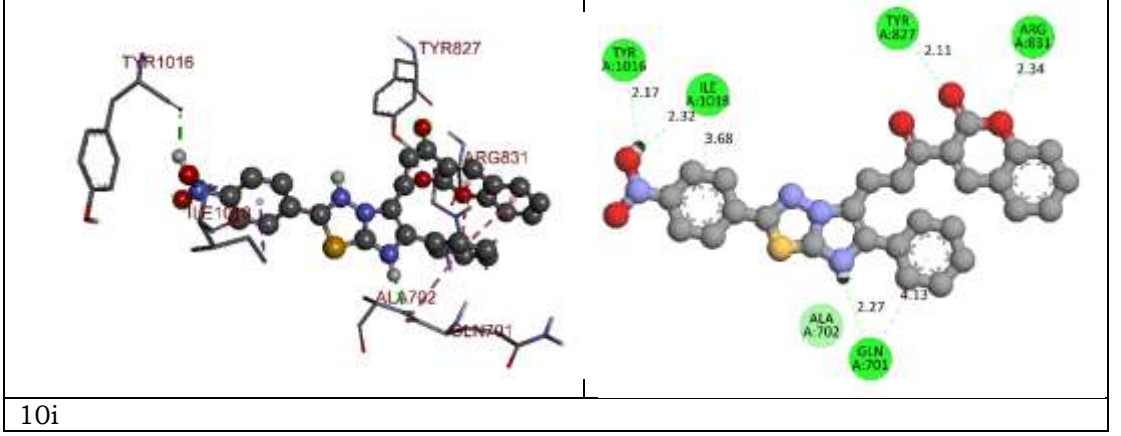
TYR1016
TYR827
ARG831
ALA792
GLN701
TYR A:827
ARG A:831
TYR A:1016
2.11
2.34
2.17
ILE A:1018
2.32
3.68
2.27
ALA A:702
GLN A:701

10i

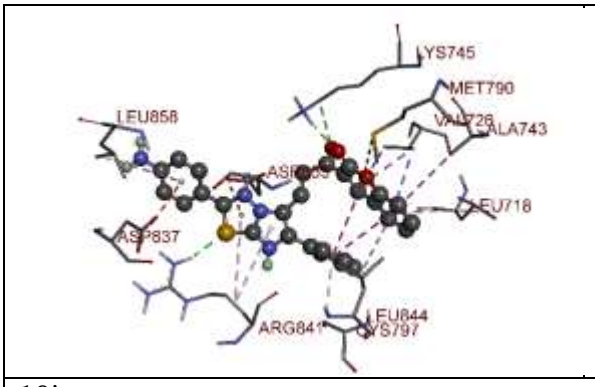
LYS745
MET790
LEU858
VAL726
ALA743
LEU718
ASP837
ARG841
LEU844
CYS797

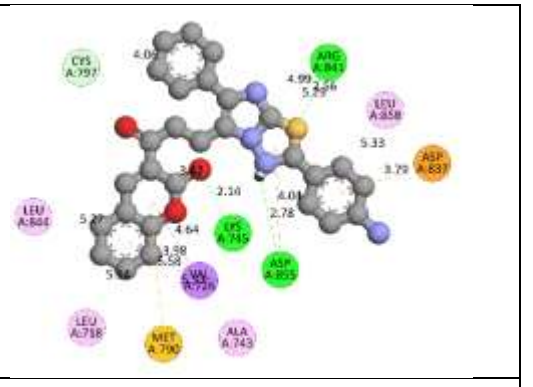

10j

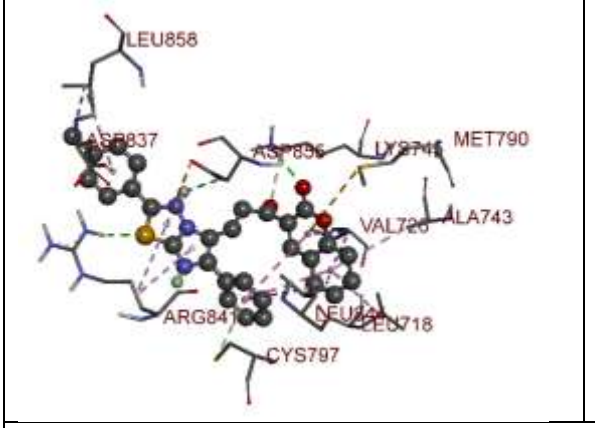
LEU858
ASP837
MET790
VAL726
ALA743
ARG841
LEU718
CYS797

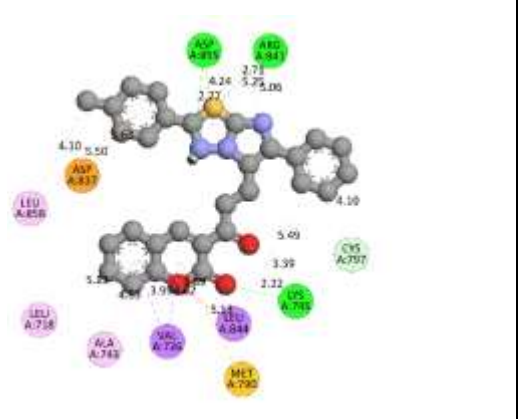

10k

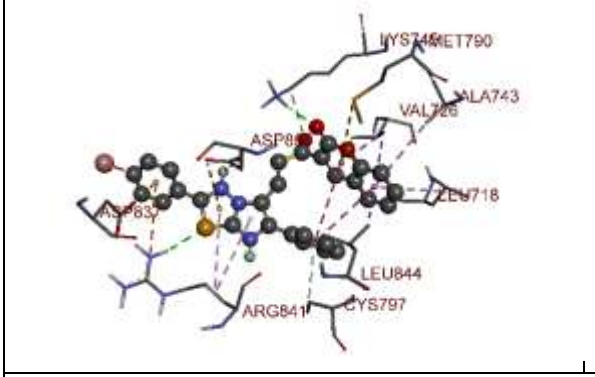
MET790
ALA743
VAL726
LEU718
ASP837
LEU844
ARG841
CYS797

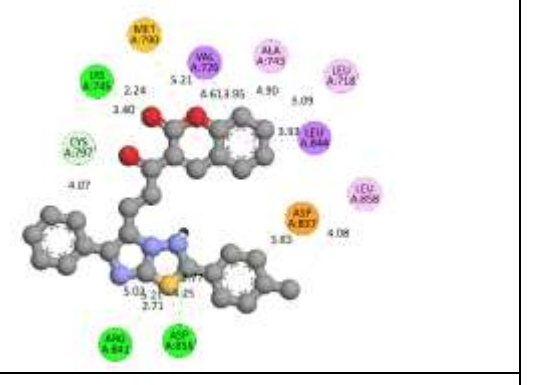

10l

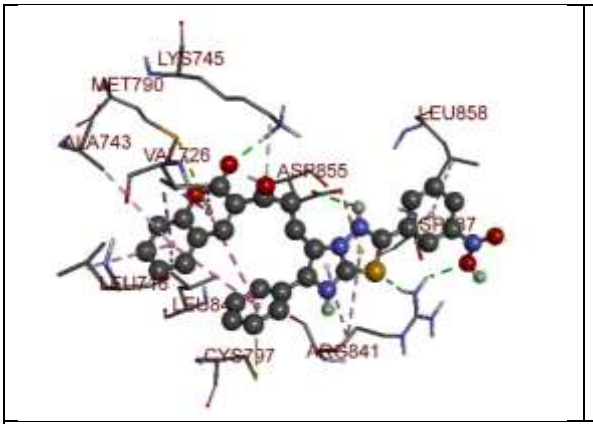
LYS745
MET790
LEU858
ALA743
VAL726
ASP855
LEU718
LEU844
CYS797
ARG841

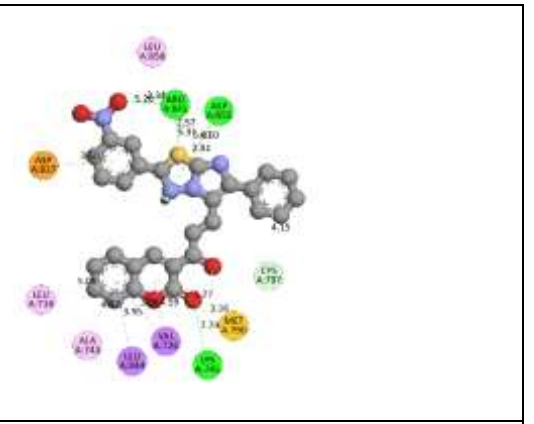

10m

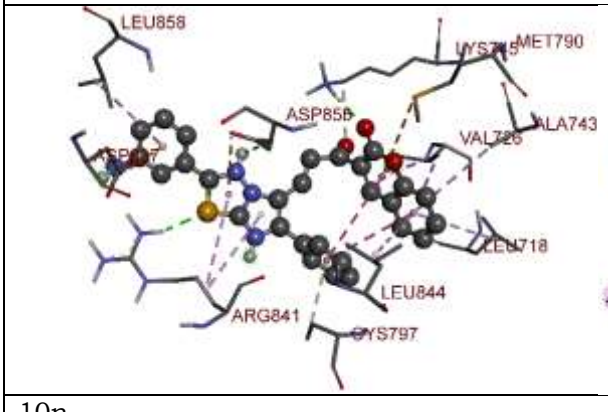
LEU858
MET790
ASP855
ALA743
VAL726
LEU718
LEU844
ARG841
CYS797

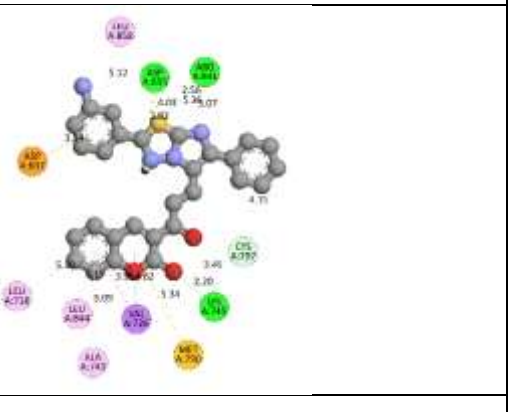

10n

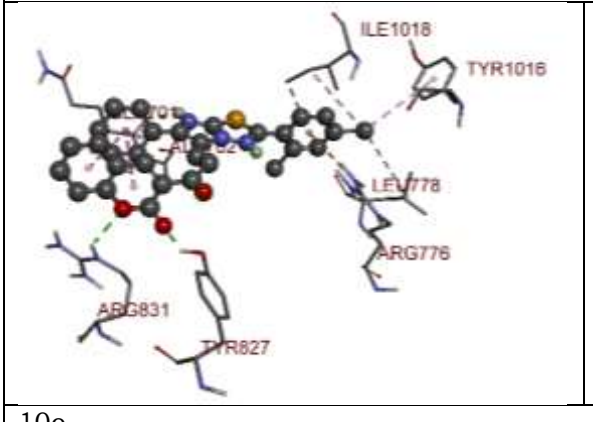
ILE1018
TYR1016
LEU778
ARG776
ARG831
TYR827

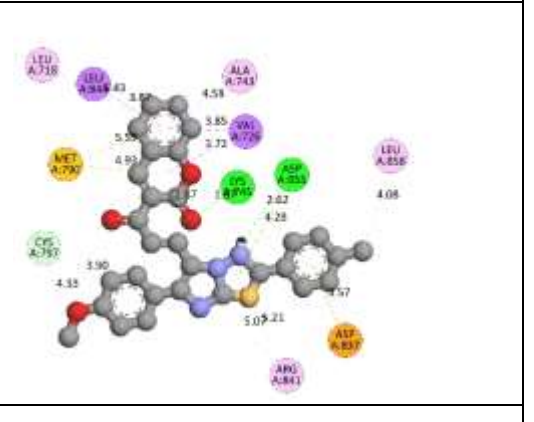

10o

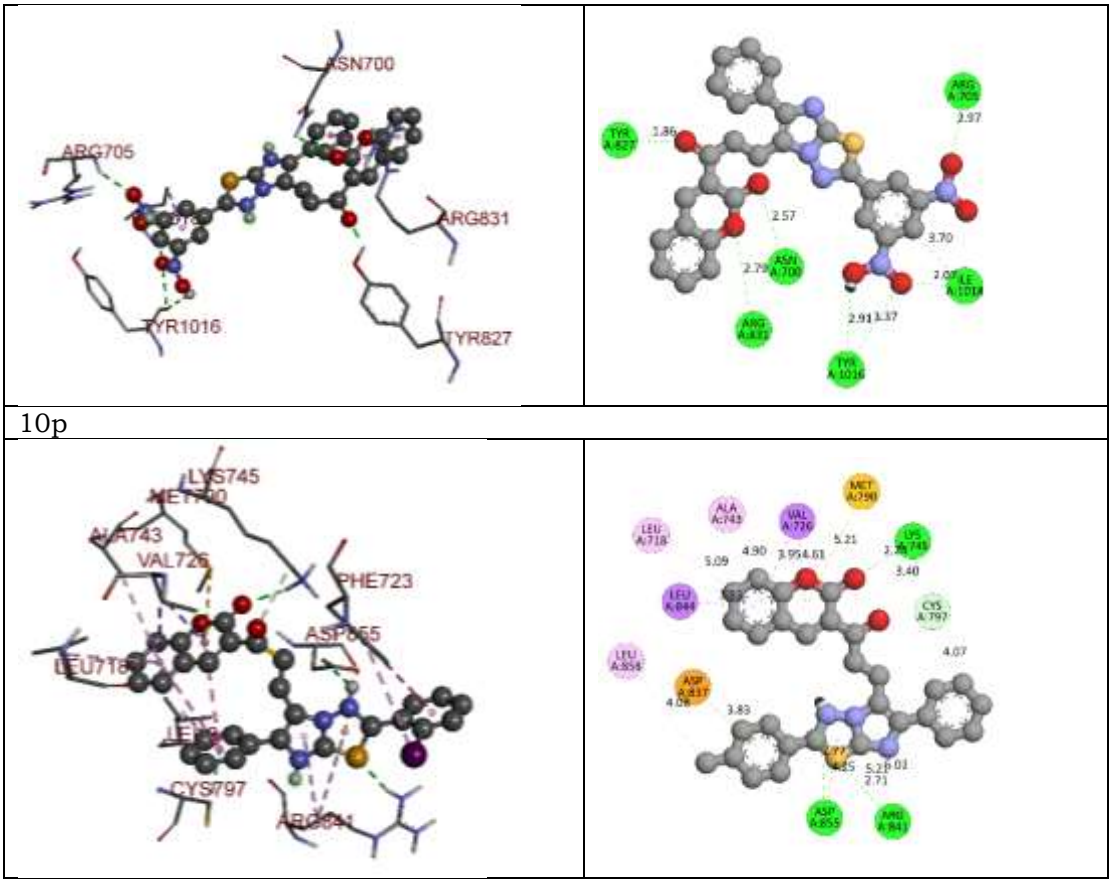

In present study, we have designed and developed some imidazo-thiadiazole based chalcone derivatives as potential EGFR inhibitors. The designed derivative were screened through molecular docking studies and subjected for synthesis followed by *in vitro* anticancer activity. The binding affinities of the derivatives have been compared with the binding mode of native ligand present in the crystal structure of EGFR enzyme (PDB ID: 5Y9T). Native ligand (naquotinib) displayed -8.3 kcal/mol binding affinity with EGFR and formed three conventional and one carbon-hydrogen bond with Gly857, Glu762, and Glu758. It has developed electrostatic (Pi-anion, attractive charge) and hydrophobic bonds (alkyl and Pi-alkyl) with Glu758, Glu762, Ala755, Pro877, and Leu858. All the designed molecules displayed most potent interactions than the native ligand.

10a exhibited -9 kcal/mol docking score and formed four conventional and one carbon-hydrogen bond with Asp855, Arg841, and Lys745. Most interestingly it has formed one Pi-donor hydrogen bond (Pi-sulfur) with Cys797 which is mutated amino acid residue for the second generation EGFR inhibitors. It has developed many hydrophobic interactions with Val726, Arg841, Leu718, Ala743, Leu844, and Leu858. It has formed Pi-sulfur bond with Met790 which is mutated amino acid residue and developed resistance to the third generation EGFR inhibitors.

10b displayed -9.3 kcal/mol binding affinity and formed four potent conventional hydrogen bonds with Asp855, Lys745, Cys797, and Arg841. It has formed one Pi-donor hydrogen bond (Pi-sulfur) with Cys797. It exhibited one Pi-anion bond with Asp837. It has developed many hydrophobic interactions with Val726, Leu844, Met790, Arg841, Leu718, Ala743, and Leu858. 10c demonstrated -9.3 kcal/mol docking score and formed three conventional and one carbon-hydrogen bond with Asp855, Lys745, and Arg841. It has formed two electrostatic bonds with Asp837 and Asp855. It has also developed many hydrophobic interactions with the amino acids same as developed by 10a and 10b. Compound 10d, 10g, & 10o displayed -9.1 kcal/mol binding affinity, formed three conventional hydrogen bonds with Asp855, Lys745 & Arg841 whereas it has developed one Pi-sigma Pi-sulfur hydrophobic bonds with Val726 and Leu844, Pi-Pi T-stacked & Pi-Alkyl hydrophobic bonds with & Arg841, Leu718, Ala743. Compound 10f exhibited -8.5 kcal/mol binding affinity, formed three conventional hydrogen bonds with Gln701, Tyr827, Arg831 whereas it has developed one Pi-sigma Pi-sulfur hydrophobic bonds with Ile1018, Pi-Pi T-stacked & Alkyl & Pi-Alkyl hydrophobic bonds with Gln701, Le1018, and Tyr1016. Compound 10m, 10n, 10p, and 10l exhibited -8.9,-8.8, -9.0 kcal/mol binding affinity, formed three conventional hydrogen bonds each with Gln701, Tyr827, and Arg831 whereas it has developed one Pi-sigma Pi-sulfur hydrophobic bonds with Ile1018, Pi-Pi T-stacked & Alkyl & Pi-Alkyl hydrophobic bonds with Gln701, Leu1018, and Met790. Compound 10g and 10j exhibited -9.1 & 9.2 kcal/mol binding affinity, formed three conventional hydrogen bonds with Gln701, Tyr827, and Arg831 whereas it has developed one Pi-sigma Pi-sulfur hydrophobic bonds with Ile1018, Pi-Pi T-stacked & Alkyl & Pi-Alkyl hydrophobic bonds with Gln701, Leu1018, and Met790.

Most interestingly many molecules had formed one Pi-donor hydrogen bond (Pi-sulfur) or conventional hydrogen bond with Cys797 which is mutated amino acid residue for the second generation EGFR inhibitors. Many molecules had formed Pi-sulfur bond with Met790 which is mutated amino acid residue and developed resistance to the third generation EGFR inhibitors. All the interaction results presented here suggest these molecule has potential to be developed as most potent 4th generation EGFR inhibitors which will might have effectiveness against triple mutant T790M/C797S EGFR. From this investigation, it was decided to synthesize all the designed molecules with their biological evaluation.

In vitro Anticancer Activity

In vitro cytotoxicity of synthesized compounds against MCF-7 (Breast cancer) and A549 (Lung cancer) cells were carried out using MTT assay. All the synthesized compounds induced the cytotoxicity to MCF-7 and A549 and displayed good range of IC_{50} values in between 4 to 59 µm/mL. Against MCF-7, out of all the tested compounds, 10a and 10e exerted good IC_{50} value i.e 4.98 and 9.66 µm/mL, respectively and compound 10c and 10d shows good IC_{50} value i.e 19.38 and 20.47 µm/mL against A549 respectively. As compared to standard it exhibited significant cytotoxic effect on tested cell lines as shown in Figure 3. The IC_{50} values of all the compounds against both cell lines are tabulated in Table 4.

Table 4. IC_{50} values of the compounds against A549 and MCF-7 cell line

Compounds	IC_{50} value	
	A549 cell line	MCF-7 cell line
10a	27.84±1.33	4.98±0.73
10b	36.36±0.39	18.24±1.07
10c	19.38±0.70	15.78±0.40
10d	20.47±2.14	11.28±0.78
10e	21.87±1.97	9.66±0.03
10f	42.55±2.50	29.91±3.88
10g	32.43±2.61	30.12±2.14
10h	25.34±2.03	48.40±11.50
10i	37.92±3.42	18.24±1.23
10j	44.62±2.23	27.55±2.38
10k	59.78±2.62	30.78±2.38
10l	30.71±1.92	34.65±2.33
10m	34.51±2.51	31.02±3.21
10n	48.61±1.52	42.43±3.92
10o	53.72±2.54	38.41±3.51
10p	28.27±0.35	49.70±1.49
Doxorubicin	3.65±0.54	4.12±0.62

The values are expressed as n=3, mean±SD.

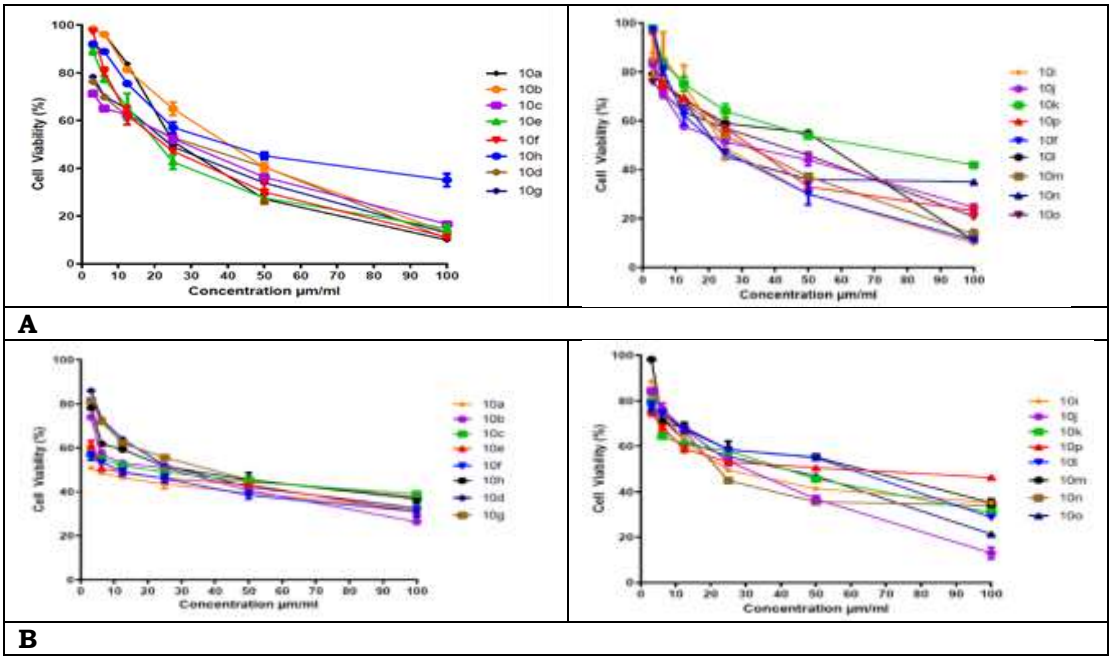

Fig. 4. A) Cell viability against A549 cell line; B) Cell viability against MFC-7 cell line

To examine whether synthesized compound induce cell death in tumor tissues we investigated the apoptosis-inducing potential of compound in MCF-7 cells using

the annexin V-FITC/PI staining technique. This method capitalizes on the binding aspects of annexin-V and PI in detecting cell death and distinguishes between its different pathways; apoptosis and necrosis using flow cytometry. The annexin V-FITC/PI staining differentiates cells into four clusters namely, live, early apoptosis, late apoptosis and necrotic cells. The untreated cells in the control sample were predominantly healthy (98.0% live cells) with only 0.0%, 0.16%, and 1.11% of the cells were in early apoptotic, late apoptotic and necrotic states. Figure 5 shows the flow cytometric evaluation of MCF-7 cells treated with synthesized compounds. The percentage of live cells decreased from 98.0% to 68.4% when treated with synthesized compound. The compound treated cells exhibited that 0.0% of the cells were in early apoptotic state and also 26.2% in late apoptotic state where 5.30% of the cells were in necrotic state. In comparison to untreated cells, synthesized compound has exhibited significant apoptosis also displayed significant apoptosis mode of death. Apoptosis study was performed and the early and late stage apoptosis results are tabulated in Table 5.

Table 5. Apoptosis examination of compound in cell line

Group	Q-4 [Live (%)]	Q-3 [Early apoptosis (%)]	Q-2 [Late apoptosis (%)]	Q-1 [Dead (%)]
Control	98.0	0.0	0.16	1.11
Sample-1	68.4	0.0	26.2	5.30

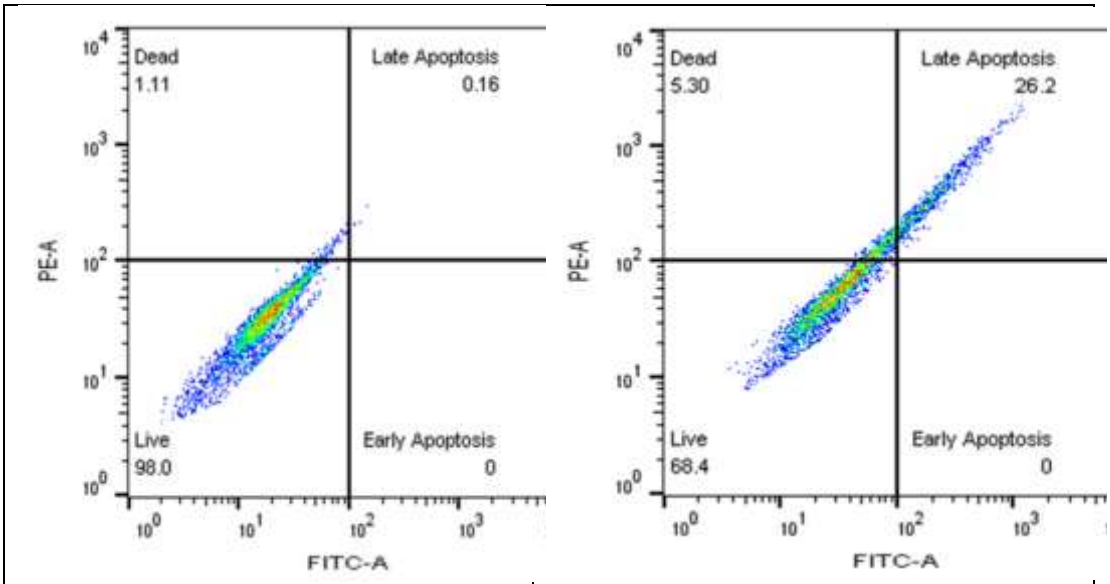

A) Untreated cell line | B) Treated cell line

Fig. 5. Apoptosis examination of compound in cell line; A) Untreated, B) Treated

Apoptosis study was performed by DAPI. Randomly the fields in the microscope was selected and counted the number of cells undergone apoptosis. Then the % of apoptic cells were calculated. The fluorescence microscopic photographs of untreated cells and cells treated with synthesized compound are shown in Figure 6. The untreated cells displayed normal intact nuclei with weak homogenous blue

staining whereas, in the treated showed small nuclei with bright chromatin condensation, blebbing, nuclear fragmentation and apoptotic bodies (small spherical fragments) formation.

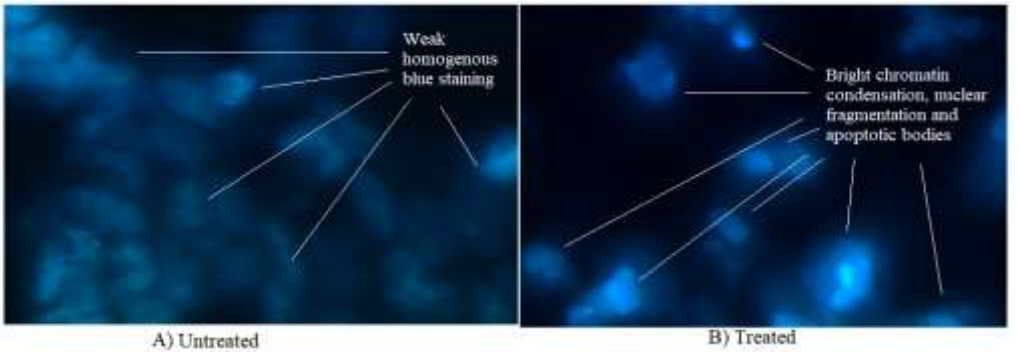

Fig. 6. The fluorescence microscopic photographs of A) Untreated cells and B) Cells treated with synthesized compound

The impact of synthesized compound on the loss of mitochondrial membrane potential M (Δ Ψ) was evaluated. After incubation, the compound-treated cells showed a significant change of mitochondria membrane potential is often to diminished green fluorescence in comparison with untreated cells emit high intensity of green fluorescence indicating collapse mitochondria membrane potential in MCF-7 cell lines as shown in Figure 7.

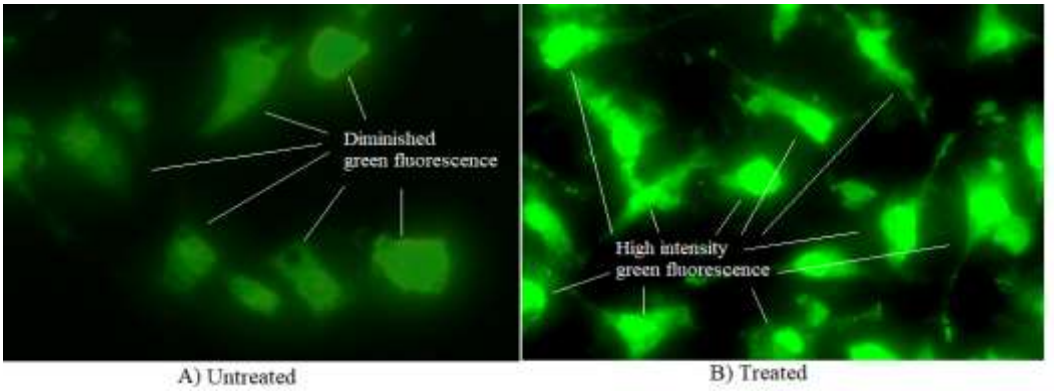

Fig. 7. Mitochondrial membrane potential; A) Untreated cell lines indicating less green fluorescence; B) Treated cell lines indicating high intensity of fluorescence

Cell cycle arrest is important mechanism in eukaryotic cells that accurately regulate cell division by monitoring defects in the cell cycle. Thus, the checkpoints permit uncontrolled cells to repair DNA damage or to consequently die by blocking cell division after DNA damage. Synthesized compound caused irreversible cell cycle arrest at the G2/M phase. For the control sample, over half of the cell population is in the G_0/G_1 phase (79.5%). There are also distinct populations of cells in the S phase (13.8%) and the G_2/M phase (4.29%). The Sub-G_1 group in the following histograms includes cellular debris and late apoptotic and necrotic cells. After treating with synthesized compound it caused a shift in

the cell population from the G_0/G_1 phase to the G_2/M phase like G_0/G_1 phase (41.4%). There were also distinct populations of cells in the S phase (9.64%) and the G_2/M phase (42.6%). Cell cycle arrest results are exemplified in Fig. 8. From the present investigation it was observed that synthesized compounds possess enough anticancer potential to treat as novel lead nucleus for the development more potent EGFR inhibitors as fourth generation inhibitors for the treatment of different cancers.

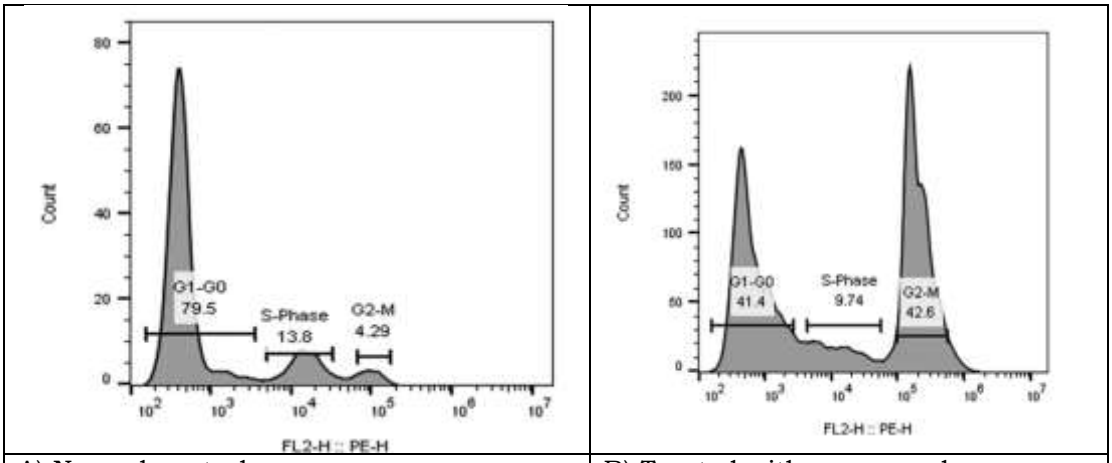

A) Normal control | B) Treated with compound

Fig. 8. Cell cycle arrest, A) Normal control; B) Treated with compound

Conclusion

In present study, we have designed and developed some imidazo-thiadiazole based chalcone derivatives as potential EGFR inhibitors. The designed derivative were screened through molecular docking studies and subjected for synthesis followed by *in vitro* anticancer activity. The binding affinities of the derivatives have been compared with the binding mode of native ligand present in the crystal structure of EGFR enzyme (PDB ID: 5Y9T). All the designed molecules displayed most potent interactions than the native ligand. Most interestingly many molecules had formed one Pi-donor hydrogen bond (Pi-sulfur) or conventional hydrogen bond with Cys797 which is mutated amino acid residue for the second generation EGFR inhibitors. Many molecules had formed Pi-sulfur bond with Met790 which is mutated amino acid residue and developed resistance to the third generation EGFR inhibitors. All the interaction results presented here suggest these molecule has potential to be developed as most potent 4th generation EGFR inhibitors which will might have effectiveness against triple mutant T790M/C797S EGFR. From this investigation, it was decided to synthesize all the designed molecules with their biological evaluation. *In vitro* cytotoxicity of synthesized compounds against MCF-7 (Breast cancer) and A549 (Lung cancer) cells were carried out using MTT assay. All the synthesized compounds induced the cytotoxicity to MCF-7 and A549. From the present investigation it was observed that synthesized compounds possess enough anticancer potential to treat as novel lead nucleus for the development more potent EGFR inhibitors as fourth generation inhibitors for the treatment of different cancers.

References

Ai, X., Guo, X., Wang, J., Stancu, A. L., Joslin, P. M. N., Zhang, D., & Zhu, S. (2018). Targeted therapies for advanced non-small cell lung cancer. *Oncotarget*, *9*(101), 37589–37607. https://doi.org/10.18632/oncotarget.26428

Akhtar, W., Khan, M. F., Verma, G., Shaquiquzzaman, M., Rizvi, M. A., Mehdi, S. H., Akhter, M., & Alam, M. M. (2017). Therapeutic evolution of benzimidazole derivatives in the last quinquennial period. *European Journal of Medicinal Chemistry*, *126*, 705–753. https://doi.org/10.1016/j.ejmech.2016.12.010

Attili, I., Karachaliou, N., Conte, P. F., Bonanno, L., & Rosell, R. (2018). Therapeutic approaches for T790M mutation positive non-small-cell lung cancer. *Expert Review of Anticancer Therapy*, *18*(10), 1021–1030. https://doi.org/10.1080/14737140.2018.1508347

Bhadoriya, K. S., Kumawat, N. K., Bhavthankar, S. V., Avchar, M. H., Dhumal, D. M., Patil, S. D., & Jain, S. V. (2016). Exploring 2D and 3D QSARs of benzimidazole derivatives as transient receptor potential melastatin 8 (TRPM8) antagonists using MLR and kNN-MFA methodology. *Journal of Saudi Chemical Society*, *20*, S256–S270. https://doi.org/10.1016/j.jscs.2012.11.001

Bhagwat, D. A., Swami, P. A., Nadaf, S. J., Choudhari, P. B., Kumbar, V. M., More, H. N., Killedar, S. G., & Kawtikwar, P. S. (2021). Capsaicin Loaded Solid SNEDDS for Enhanced Bioavailability and Anticancer Activity: In-Vitro, In-Silico, and In-Vivo Characterization. *Journal of Pharmaceutical Sciences*, *110*(1), 280–291. https://doi.org/10.1016/j.xphs.2020.10.020

Bryce, A. H., Rao, R., Sarkaria, J., Reid, J. M., Qi, Y., Qin, R., James, C. D., Jenkins, R. B., Boni, J., Erlichman, C., & Haluska, P. (2012). Phase i study of temsirolimus in combination with EKB-569 in patients with advanced solid tumors. *Investigational New Drugs*, *30*(5), 1934–1941. https://doi.org/10.1007/s10637-011-9742-1

Chan, D. L. H., Segelov, E., Wong, R. S. H., Smith, A., Herbertson, R. A., Li, B. T., Tebbutt, N., Price, T., & Pavlakis, N. (2017). Epidermal growth factor receptor (EGFR) inhibitors for metastatic colorectal cancer. In *Cochrane Database of Systematic Reviews* (Vol. 2017, Issue 6). https://doi.org/10.1002/14651858.CD007047.pub2

Chaudhari, R. N., Khan, S. L., Chaudhary, R. S., Jain, S. P., & Siddiqui, F. A. (2020). B-Sitosterol: Isolation from Muntingia Calabura Linn Bark Extract, Structural Elucidation And Molecular Docking Studies As Potential Inhibitor of SARS-CoV-2 Mpro (COVID-19). *Asian Journal of Pharmaceutical and Clinical Research*, *13*(5), 204–209. https://doi.org/10.22159/ajpcr.2020.v13i5.37909

Chen, L., Fu, W., Zheng, L., Liu, Z., & Liang, G. (2018). Recent Progress of Small-Molecule Epidermal Growth Factor Receptor (EGFR) Inhibitors against C797S Resistance in Non-Small-Cell Lung Cancer. In *Journal of Medicinal Chemistry* (Vol. 61, Issue 10, pp. 4290–4300). https://doi.org/10.1021/acs.jmedchem.7b01310

Dallakyan, S., & Olson, A. J. (2015). Small-molecule library screening by docking with PyRx. *Methods in Molecular Biology*, *1263*(1263), 243–250. https://doi.org/10.1007/978-1-4939-2269-7_19

Galayev, O., Garazd, Y., Garazd, M., & Lesyk, R. (2015). Synthesis and anticancer activity of 6-heteroarylcoumarins. *European Journal of Medicinal Chemistry*, *105*, 171–181. https://doi.org/10.1016/j.ejmech.2015.10.021

Ghorab, M. M., Ragab, F. A., Heiba, H. I., El-Gazzar, M. G., & Zahran, S. S.

(2015). Synthesis, anticancer and radiosensitizing evaluation of some novel sulfonamide derivatives. *European Journal of Medicinal Chemistry*, *92*, 682–692. https://doi.org/10.1016/j.ejmech.2015.01.036

Gil, A., Pabón, A., Galiano, S., Burguete, A., Pérez-Silanes, S., Deharo, E., Monge, A., & Aldana, I. (2014). Synthesis, biological evaluation and structure-activity relationships of new quinoxaline derivatives as anti-Plasmodium falciparum agents. *Molecules*, *19*(2), 2166–2180. https://doi.org/10.3390/molecules19022166

Gokhale, N., Dalimba, U., & Kumsi, M. (2017). Facile synthesis of indole-pyrimidine hybrids and evaluation of their anticancer and antimicrobial activity. *Journal of Saudi Chemical Society*, *21*(7), 761–775. https://doi.org/10.1016/j.jscs.2015.09.003

Grünwald, V., & Hidalgo, M. (2003a). Developing inhibitors of the epidermal growth factor receptor for cancer treatment. In *Journal of the National Cancer Institute* (Vol. 95, Issue 12, pp. 851–867). https://doi.org/10.1093/jnci/95.12.851

Grünwald, V., & Hidalgo, M. (2003b). Developing inhibitors of the epidermal growth factor receptor for cancer treatment. *Journal of the National Cancer Institute*, *95*(12), 851–867. https://doi.org/10.1093/jnci/95.12.851

Harari, P. M. (2004). Epidermal growth factor receptor inhibition strategies in oncology. In *Endocrine-Related Cancer* (Vol. 11, Issue 4, pp. 689–708). https://doi.org/10.1677/erc.1.00600

Khan, Sharuk L; Siddiui, F. A. (2020). Beta-Sitosterol: As Immunostimulant, Antioxidant and Inhibitor of SARS-CoV-2 Spike Glycoprotein. *Archives of Pharmacology and Therapeutics*, *2*(1). https://doi.org/10.33696/pharmacol.2.014

Khan, A., Unnisa, A., Sohel, M., Date, M., Panpaliya, N., Saboo, S. G., Siddiqui, F., & Khan, S. (2022). Investigation of phytoconstituents of Enicostemma littorale as potential glucokinase activators through molecular docking for the treatment of type 2 diabetes mellitus. *In Silico Pharmacology*, *10*(1). https://doi.org/10.1007/s40203-021-00116-8

Khan, S., Kale, M., Siddiqui, F., & Nema, N. (2021). Novel pyrimidine-benzimidazole hybrids with antibacterial and antifungal properties and potential inhibition of SARS-CoV-2 main protease and spike glycoprotein. *Digital Chinese Medicine*, *4*(2), 102–119. https://doi.org/10.1016/j.dcmed.2021.06.004

Khan, S.L., Siddiqui, F. A., Jain, S. P., & Sonwane, G. M. (2020). Discovery of Potential Inhibitors of SARS-CoV-2 (COVID-19) Main Protease (Mpro) from Nigella Sativa (Black Seed) by Molecular Docking Study. *Coronaviruses*, *2*(3), 384–402. https://doi.org/10.2174/2666796701999200921094103

Khan, Sharuk L., Siddiqui, F. A., Shaikh, M. S., Nema, N. V., & Shaikh, A. A. (2021). Discovery of potential inhibitors of the receptor-binding domain (RBD) of pandemic disease-causing SARS-CoV-2 Spike Glycoprotein from Triphala through molecular docking. *Current Chinese Chemistry*, *01*. https://doi.org/10.2174/2666001601666210322121802

Khan, Sharuk L., Sonwane, G. M., Siddiqui, F. A., Jain, S. P., Kale, M. A., & Borkar, V. S. (2020). Discovery of Naturally Occurring Flavonoids as Human Cytochrome P450 (CYP3A4) Inhibitors with the Aid of Computational Chemistry. *Indo Global Journal of Pharmaceutical Sciences*, *10*(04), 58–69. https://doi.org/10.35652/igjps.2020.10409

Kumbar, V. M., Peram, M. R., Kugaji, M. S., Shah, T., Patil, S. P., Muddapur, U. M., & Bhat, K. G. (2021). Effect of curcumin on growth, biofilm formation and virulence factor gene expression of Porphyromonas gingivalis. *Odontology*, *109*(1), 18–28. https://doi.org/10.1007/s10266-020-00514-y

Lv, P. C., Li, D. D., Li, Q. S., Lu, X., Xiao, Z. P., & Zhu, H. L. (2011). Synthesis, molecular docking and evaluation of thiazolyl-pyrazoline derivatives as EGFR TK inhibitors and potential anticancer agents. *Bioorganic and Medicinal Chemistry Letters*, *21*(18), 5374–5377. https://doi.org/10.1016/j.bmcl.2011.07.010

Mohana Roopan, S., & Sompalle, R. (2016). Synthetic chemistry of pyrimidines and fused pyrimidines: A review. *Synthetic Communications*, *46*(8), 645–672. https://doi.org/10.1080/00397911.2016.1165254

Peram, M. R., Jalalpure, S., Kumbar, V., Patil, S., Joshi, S., Bhat, K., & Diwan, P. (2019). Factorial design based curcumin ethosomal nanocarriers for the skin cancer delivery: in vitro evaluation. *Journal of Liposome Research*, *29*(3), 291–311. https://doi.org/10.1080/08982104.2018.1556292

Rappé, A. K., Casewit, C. J., Colwell, K. S., Goddard, W. A., & Skiff, W. M. (1992). UFF, a Full Periodic Table Force Field for Molecular Mechanics and Molecular Dynamics Simulations. *Journal of the American Chemical Society*, *114*(25), 10024–10035. https://doi.org/10.1021/ja00051a040

Roskoski, R. (2016). Cyclin-dependent protein kinase inhibitors including palbociclib as anticancer drugs. *Pharmacological Research*, *107*, 249–275. https://doi.org/10.1016/j.phrs.2016.03.012

Saavedra, L. M., Ruiz, D., Romanelli, G. P., & Duchowicz, P. R. (2015). Quantitative Structure-Antifungal Activity Relationships for cinnamate derivatives. *Ecotoxicology and Environmental Safety*, *122*, 521–527. https://doi.org/10.1016/j.ecoenv.2015.09.024

San Diego: Accelrys Software Inc. (2012). Discovery Studio Modeling Environment, Release 3.5. *Accelrys Software Inc.* https://www.3dsbiovia.com/about/citations-references/

Shntaif, A. H., Khan, S., Tapadiya, G., Chettupalli, A., Saboo, S., Shaikh, M. S., Siddiqui, F., & Amara, R. R. (2021). Rational drug design, synthesis, and biological evaluation of novel N-(2-arylaminophenyl)-2,3-diphenylquinoxaline-6-sulfonamides as potential antimalarial, antifungal, and antibacterial agents. *Digital Chinese Medicine*, *4*(4), 290–304. https://doi.org/10.1016/j.dcmed.2021.12.004

Siddiqui, F. A., Khan, S. L., Marathe, R. P., & Nema, N. V. (2021). Design, Synthesis, and In Silico Studies of Novel N-(2-Aminophenyl)-2,3-Diphenylquinoxaline-6-Sulfonamide Derivatives Targeting Receptor- Binding Domain (RBD) of SARS-CoV-2 Spike Glycoprotein and their Evaluation as Antimicrobial and Antimalarial Agents. *Letters in Drug Design & Discovery*, *18*(9), 915–931. https://doi.org/10.2174/1570180818666210427095203

Song, Z., Ge, Y., Wang, C., Huang, S., Shu, X., Liu, K., Zhou, Y., & Ma, X. (2016). Challenges and perspectives on the development of small-molecule EGFR inhibitors against T790M-mediated resistance in non-small-cell lung cancer: Miniperspective. In *Journal of Medicinal Chemistry* (Vol. 59, Issue 14, pp. 6580–6594). https://doi.org/10.1021/acs.jmedchem.5b00840

Woodburn, J. R. (1999). The epidermal growth factor receptor and its inhibition in cancer therapy. *Pharmacology and Therapeutics*, *82*(2–3), 241–250. https://doi.org/10.1016/S0163-7258(98)00045-X

Widana, I.K., Dewi, G.A.O.C., Suryasa, W. (2020). Ergonomics approach to improve student concentration on learning process of professional ethics. *Journal of Advanced Research in Dynamical and Control Systems*, *12*(7), 429-445.

Widana, I.K., Sumetri, N.W., Sutapa, I.K., Suryasa, W. (2021). Anthropometric measures for better cardiovascular and musculoskeletal health. *Computer Applications in Engineering Education*, *29*(3), 550–561. https://doi.org/10.1002/cae.22202